Front. Phys. 13(4), 136106 (2018)
https://doi.org/10.1007/s11467-018-0792-0

RESEARCH ARTICLE

Novel single-walled carbon nanotubes periodically embedded with four- and eight-membered rings

Xiao-Ning Wang[1], Jun-Zhe Lu[1,2,†], Heng-Jiang Zhu[1,2,‡], Fang-Fang Li[1], Miao-Miao Ma[1], Gui-Ping Tan[1]

[1] *College of Physics and Electronic Engineering, Xinjiang Normal University, Urumqi 830054, China*
[2] *Key Laboratory of Mineral Luminescence Materials and Microstructures of Xinjiang Uygur Autonomous Region, Urumqi 830054, China*
Corresponding authors. E-mail: [†] *723678610@qq.com,* [‡] *zhj@xjnu.edu.cn*
Received December 21, 2017; accepted April 15, 2018

Based on experimental results, we obtain five types of single-walled carbon nanotube (SWNT) clusters with different chirality indices and diameters using density functional theory (DFT). We then obtain the corresponding SWNTs by using periodic boundary conditions. Studies of the stability and electronic properties show that the stability of the novel SWNTs is independent of the chirality index and relates only to the tube diameter; larger diameters correspond to more stable SWNTs. The electronic properties all show metallic characteristics independent of the chirality indices and tube diameters, thereby promoting the application of metallic-type SWNTs.

Keywords four- and eight-membered rings, novel SWNTs, stability, electronic properties

PACS numbers 61.48.De, 65.80.-g, 61.46.Bc, 61.46.-W

1 Introduction

Materials with at least one dimension in the range 1–100 nm are called nanomaterials. Recently, carbon nanotubes (CNTs) have become regarded as quasi-one-dimensional nanomaterials with broad application prospects arising from their unique structures and physicochemical properties [1, 2]. The arrangements of C atoms in the honeycomb grids on the surfaces of single-walled CNTs (SWNTs) have helicity [3]. Because of the helicity and the significant differences in electronic states induced by varying diameters, SWNTs can show either metallic or semiconducting electronic properties [4–6]. Metallic SWNTs (m-SWNTs) have become typical model systems for studying various quantum phenomena in quasi-one-dimensional solid-state systems [7], including single-electron conduction, Luttinger liquids, weak delocalization effects, ballistic transmission, and quantum interference. Semiconductive SWNTs (s-SWNTs) are used to build new types of nanoelectronic devices such as transistors, logic devices, memory devices, and sensing devices [8]. In addition, the superb tensile strength of SWNTs permits their use as reinforcing fibers and polymeric additives for various structural materials. Furthermore, because they have high specific surface areas and strong absorption features, SWNTs can also be used as hydrogen storage and energy storage materials [3]. The thermodynamic properties of CNTs and their compatibility with biological systems have inspired widespread interest in CNT applications in the field of cancer diagnosis and treatment [9].

At present, SWNTs obtained using various experimental methods implemented by macroscopic preparation show both metallic and semiconductive properties, which prevents the useful application of the CNTs [10, 11]. However, in the last two decades, SWNTs with pure single-type electronic properties have been obtained by controlling their structures during experimental preparation or by separating m-SWNTs and s-SWNTs completely [11–14].

In experiments, Yang's group has achieved the high-purity preparation of $(12, 6)$ and $(16, 0)$ SWNTs by controlling the structure of the catalyst through chemical vapor deposition (CVD), with purities reaching 92% and 79.2%, respectively [3, 15, 16]. In 2008, Tanaka *et al.* first proposed an agarose gel electrophoresis method to separate s-SWNTs and m-SWNTs, obtaining 95% and 70% purities, respectively [11]. Liu *et al.* successfully realized the simultaneous separation of m- and s-SWNTs

and diameter-selective SWNTs enrichment by gel chromatography [14]. Yahya *et al.* exploited a gel agarose microbead filtration technique to achieve 70% m-SWNTs and > 95% s-SWNTs [13].

In theoretical studies, Terrones *et al.* proposed a chirality- and diameter-independent m-SWNTs family with ordered pentagonal, hexagonal, and heptagonal metal sheets [17, 18]. Based on penta-graphene, Zhang et al. obtained SWNTs of almost purely semiconducting natures by using a five-membered carbocyclic ring as the structural unit [19].

So far, the issue of obtaining SWNTs with single-type electronic properties remains fundamentally unsolved. Therefore, it is of great practical significance to explore or prepare SWNTs with single-type electronic properties, both theoretically and experimentally, to enable the effective application of SWNTs [20].

In 2013, Algara-Siller *et al.* used electron-beam engineering to obtain double-walled carbon nanoribbons by cutting double-layer graphene for the successful preparation of SWNTs [21]. In 2016, Xu *et al.* used the same method to cut bilayer boron nitride (BN) nanosheets and connected two BN nanoribbons at the cutting edges to obtain the smallest $(3, 3)$ BN nanotubes yet reported [22]. The greatest advantages of nanotube electron-beam engineering are the controllability and repeatability of the preparation process [22].

In March 2017, Liu *et al.* successfully fabricated graphene-like nanoribbons periodically embedded with four- and eight-membered rings for the first time [23]. By scanning tunneling spectroscopy and density functional theory (DFT), they found that four- and eight-membered rings as topological defects effectively changed the electronic properties of the nanoribbons and confirmed that non-six-membered rings also effectively controlled the structures of the nanobelts [23].

By considering the above related theoretical and experimental studies, and from the isomer perspective, we assume that via electron-beam engineering, novel SWNTs with different diameters and embedded with periodic four- and eight-membered rings can be prepared by cutting bilayer graphene-like nanoribbons of predetermined widths. Therefore, in this study, we have investigated new isomers of SWNTs with periodically embedded four- and eight-membered rings, with the intent to obtain SWNTs with single-type electronic properties and provide new ideas for the experimental preparation of SWNTs with single-type electronic properties.

2 Methods and details

In previous studies, researchers used the GAUSSIAN03 package with B3LYP/3-21G methods to study CNTs with six-membered rings, and obtained theoretical results consistent with reported experimental results [24, 25]. Therefore, in this study we calculate the related properties of the novel SWNTs using B3LYP/3-21G methods to optimize the calculation of tubular clusters. Because the PBEPBE functional is more suitable for large systems, PBEPBE/6-31G is chosen to calculate the electronic properties of the novel SWNTs under periodic boundary conditions (PBC). Here, we note that during the calculation, we always consider the computational efficiency and accuracy of our method.

The energy band structures of the SWNTs are calculated by selecting 240 K-points and the electronic density of states (DOS) are calculated while the full width at half maximum (FWHM) is 0.3 eV. During the calculation processes, the convergence criterion is 10^{-6} atomic units (a.u.).

As indicated in a recent work [20], SWNTs comprising six-membered rings can be viewed as curled graphene sheets having six-membered rings as the structural unit. Thus, the novel SWNTs can be regarded as the curling of graphene embedded with periodic four- and eight-membered rings. As shown in Fig. 1, the chirality indices of the novel SWNTs are similar to those of six-membered-ring SWNTs [20], defined as $\boldsymbol{C}_h = n\boldsymbol{a}_1 + m\boldsymbol{a}_2$. In this case, the lengths of the base vectors $\boldsymbol{a}_1$ and $\boldsymbol{a}_2$ are different and perpendicular to each other, unlike six-membered ring chirality indices. In particular, the four- and eight-membered rings with different distributions in the tube walls yield five types of novel SWNTs, represented as $(n, 0)$, $(0, m)$, (n, n), and (n, m) $(n > m,$ $n < m)$, respectively. The corresponding tubular clusters are denoted as $[n, 0]$, $[0, m]$, $[n, n]$, and $[n, m]$ $(n > m,$ $n < m)$.

Because the coordination number of each C atom is three, if the coordination numbers of C atoms at the tube end are not satisfied, the corresponding tubular C

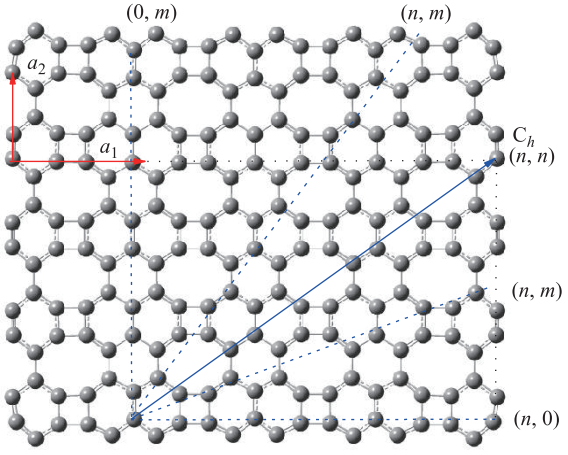

Fig. 1 Graphene periodically embedded with four- and eight-membered rings and chirality indices.

clusters will be unstable [26–30]. Therefore, this study adopts H passivation, in which H atoms are attached to the C atoms at the tube end, to optimize and calculate the frequency, and to obtain stable configurations with no imaginary-frequency distributions in the tubular C clusters.

3 Results and discussion

3.1 Novel SWNT clusters periodically embedded with four- and eight-membered rings

In this study, we obtain the five stable tubular cluster types of $[n,0]$, $[0,m]$, $[n,n]$, and $[n,m]$ ($n > m$, $n < m$) without any imaginary frequencies. Among them, n and m vary from 0 to 6. Figure 2 shows the structural characteristics of tubular clusters; the four- and eight-membered rings in $[n,0]$ are distributed periodically along the busbars (Straight line on the pipe wall which parallel to the axis). In $[n,0]$, $[n,n-1]$, and $[m-1,m]$, the four- and eight-membered rings show spiral distributions along the pipe wall. The distribution of four- and eight-membered rings in $[n,n-1]$ is a left-handed spiral, while that in $[n,n]$ and $[m-1,m]$ is right-handed. In addition, the helicity values of $[m-1,m]$ and $[n,n-1]$ are larger than that of $[n,n]$.

3.2 Thermodynamic stability

The stability of the cluster structure can be determined by the relationship between the structure and temperature (as in molecular dynamics methods), or by the frequency of intrinsic vibrations. The structure is stable only if it does not disintegrate with increasing temperature. In order to further investigate the stability of the SWNT clusters, we check the thermodynamic stability using parameters including the internal energy (E_T), entropy (S), and constant-volume heat capacity (C_V) of the clusters based on structural optimization and frequency calculation without any imaginary frequency. Figure 3 shows that, as the temperature increases, E_T and S increase continuously, which agrees with the laws of thermodynamics and indicates that our calculated results are reliable. In particular, C_V reaches the Dulong–Petit limit as the temperature increases; after this limit, C_V is independent of temperature. This result indicates that the structure does not disintegrate with increasing temperature, i.e., the structure is thermodynamically stable.

3.3 Novel SWNTs

Figure 4 shows the novel SWNTs obtained by PBC and their smallest repeating units, which are selected from the corresponding tubular clusters. The PBEPBE/6-31G method is selected to optimize these structures.

As predicted in the theoretical results, non-hexagonal C rings induce changes in the local density of π-electron, electronic structures, and magnetic properties of graphene-like nanoribbons [31–33]. To study the influence of four- and eight-membered C rings, we have performed DFT calculations to further investigate the effects of four- and eight-membered rings on the geometric structures and electronic properties of the novel SWNTs. As shown in Fig. 4, our results are consistent with those in Ref. [2]; with the absence of hexagonal symmetry (Fig. 4) [34], the C–C bonds in the non-hexagonal rings are shortened or lengthened in the range 1.39–1.52 Å, while the C–C–C angles vary within the range 89°–145°.

3.4 Formation energy of novel SWNTs

According to the method of electron-beam engineering, the novel SWNTs can be successfully prepared by cutting

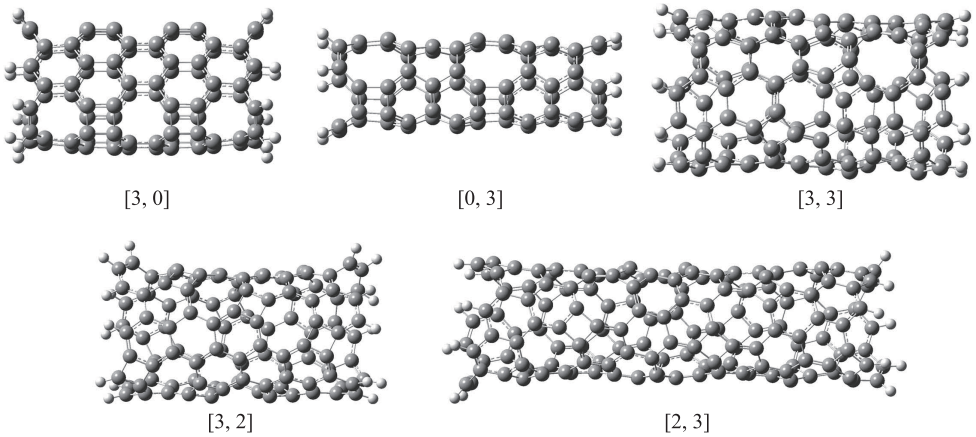

Fig. 2 The $[3,0]$, $[0,3]$, $[3,3]$, $[3,2]$, and $[2,3]$ novel single-walled carbon nanotube clusters.

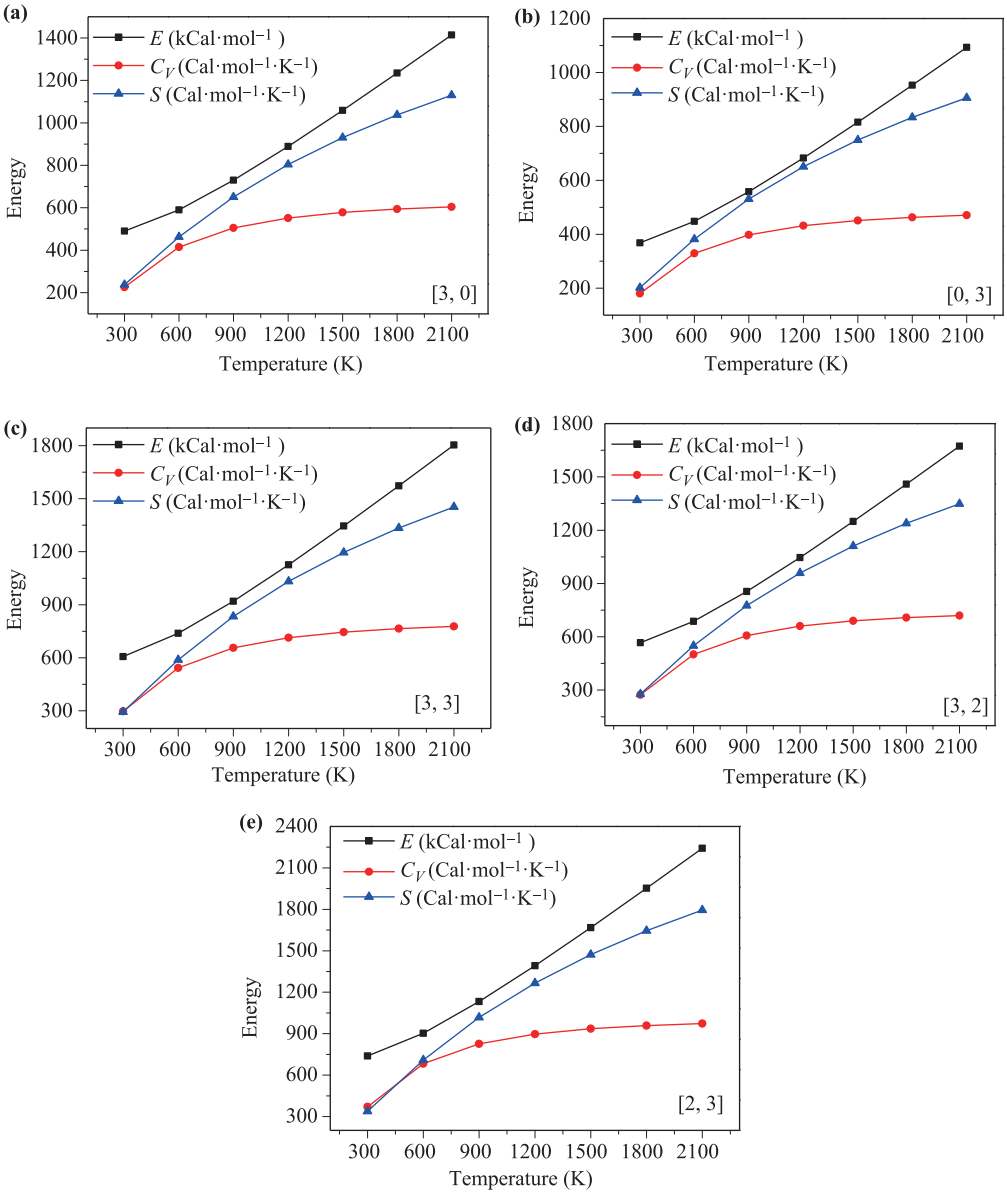

Fig. 3 Here, **(a–e)** for [3, 0], [0, 3], [3, 3], [3, 2], and [2, 3], with changing the thermodynamic quantities at different temperatures, respectively.

double-layer graphene-like nanoribbons of predetermined width with embedded four- and eight-membered rings. Therefore, we calculate the formation energies of the SWNTs corresponding to the double-layered graphene-like nanoribbons as [35, 36]

$$E_{\text{formation}} = \frac{E_T(SWNTs) - 2E_T(nanoribbons)}{k}.$$

Here, E_T (SWNTs) is the energy of one repeating unit of the SWNT, E_T (nanoribbons) is the energy of one repeating unit in the nanoribbon, k is the number of C atoms in one repeating unit of the SWNT, and $k/2$ is the number of C atoms in one repeating unit of the nanoribbon. As shown in Table 1, the energy of a single SWNT or double-walled nanoribbon is negative, and the energy of the SWNT is always lower than that of the corresponding double-walled nanoribbon. The formation energy of the novel SWNTs is negative, indicating that forming SWNTs from nanoribbons is an easy exothermic reaction.

3.5 Energy stability of novel SWNTs

The average binding energy (E_b) of the novel SWNTs is defined as the average energy released when C atoms are incorporated into the SWNTs. A greater energy release

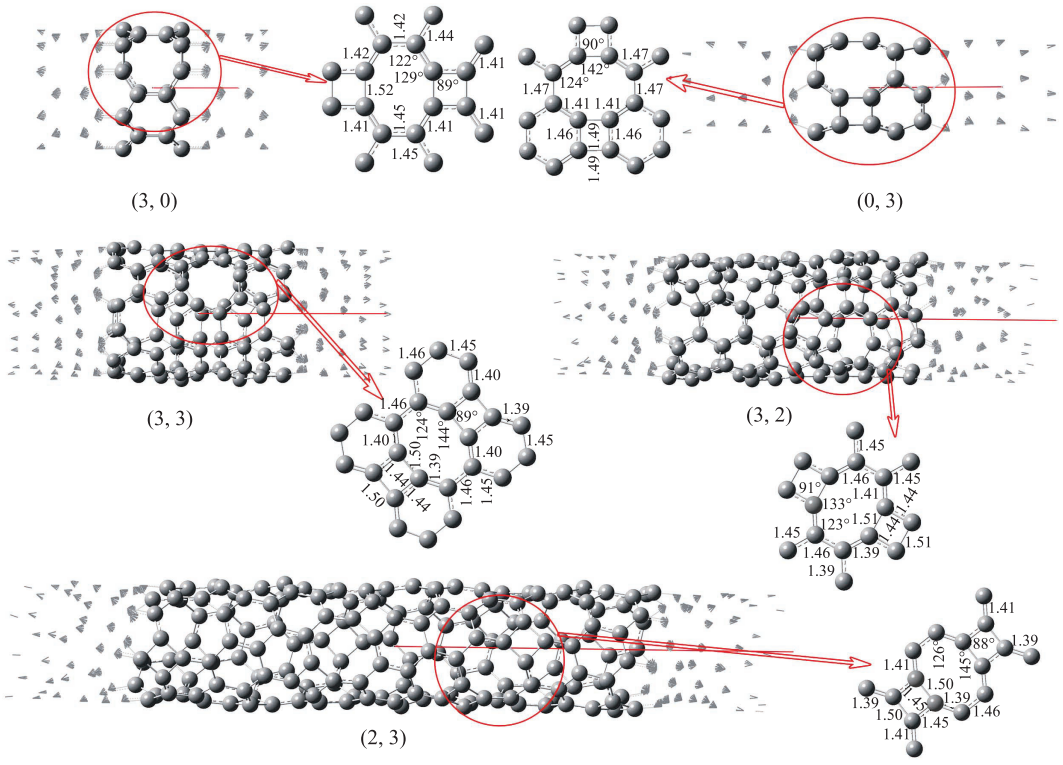

Fig. 4 The structures, bonds, and angles of repeat unit.

Table 1 Formation energy of the novel SWNTs.

	(0, 2)	(0, 3)	(0, 4)	(0, 5)	(0, 6)
E_T (SWNTs)/eV	−20692.5	−31053.1	−41411.2	−51768.1	−62124.4
E_T (nanoribbons)/eV	−10342.6	−15521.6	−20697.7	−25874.5	−31052
k	20	30	40	50	60
$E_{formation}$ (eV·atom^{-1})	−0.3678	−0.3299	−0.39422	−0.38074	−0.33824

corresponds to greater SWNT stability. The formula is

$$E_b = \frac{kE(C) - E(C_k)}{k}.$$

Here, $E(C)$ represents the C atom energy, and $E(C_k)$ represents the energy of the novel SWNT, respectively. Because of the base vector $|\boldsymbol{a}_1| > |\boldsymbol{a}_2|$, the relationship between the diameter values d of the novel SWNTs are as follows: $d_{(n,n)} > d_{(n,0)} > d_{(0,m)}$ and $d_{(n,n)} > d_{(n,n-1)} > d_{(m-1,m)}$ when $m = n > 2$. However, when $m = n = 2$, an abnormality occurs: $d_{(n,0)} > d_{(n,n-1)} > d_{(m-1,m)}$, possibly because the novel $(n, n-1)$ and $(m-1, m)$ SWNTs with small diameters possess too many folds. It can be seen from Fig. 5 that the E_b of SWNTs with equal chirality indices is increased as the diameter d increases and finally stabilizes, that is, for SWNTs of the same chirality indices, larger diameters correspond to more stable SWNTs. The E_b of SWNTs with different chirality indices is increased with increasing tube diameter, approaching the same stable value as that for equal-indices SWNTs. In other words, for SWNTs with different chi-

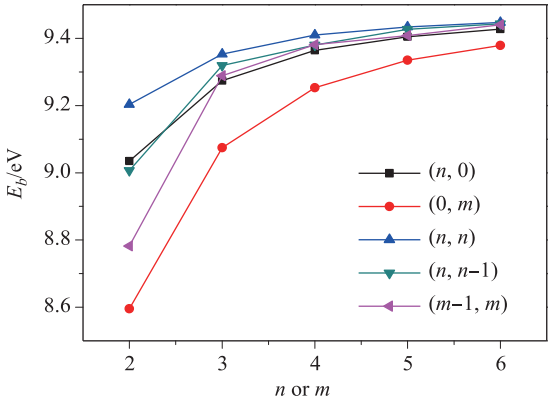

Fig. 5 The average binding energy of novel SWNTs varies with n or m.

rality indices, the SWNTs also increase in stability with larger diameters. This indicates that the preparation of larger-diameter novel SWNTs is more easily achieved because of their improved stability.

3.6 Electronic properties of novel SWNTs

The PBEPBE/6-31G functional is chosen to calculate the electronic properties of SWNTs by using PBC. Among them, the energy band structures of the novel SWNTs are calculated by selecting 240 K-points, and the electronic DOS is calculated when the FWHM is 0.3 eV.

Table 2 shows the highest occupied crystal orbital (HOCO)/lowest unoccupied crystal orbital (LUCO) energies, indirect band gap, and minimum direct band gap for the novel SWNTs. As shown in Table 2, the novel SWNTs have very small or zero energy gaps and exhibit metallic properties.

Table 2 Electronic properties of the novel SWNTs.

SWNT	HOCO (eV)	LUCO (eV)	Indirect gap (eV)	Min direct Gap (eV)
(2, 0)	−4.6375	−4.9356	−0.2981	0.0019
(3, 0)	−4.1990	−4.5422	−0.3432	0.0008
(4, 0)	−4.4441	−4.4346	0.0095	0.0095
(5, 0)	−4.3015	−4.6288	−0.3272	0.0001
(6, 0)	−4.4007	−4.4275	−0.0268	0.0148
(0, 2)	−4.7475	−4.6541	0.0934	0.3344
(0, 3)	−3.9535	−5.0382	−1.0848	0.0003
(0, 4)	−4.0044	−5.0519	−1.0475	0.0008
(0, 5)	−3.8576	−5.0710	−1.2134	0.0004
(0, 6)	−3.8869	−5.0167	−1.1298	0.0004
(2, 2)	−4.1311	−4.8403	−0.7092	0.0020
(3, 3)	−3.9619	−4.4956	−0.5337	0.0044
(4, 4)	−3.9096	−4.8644	−0.9548	0.0003
(5, 5)	−3.8721	−4.8574	−0.9853	0.0002
(6, 6)	−3.8537	−4.8504	−0.9967	0.0004
(2, 1)	−4.4255	−4.7134	−0.2878	0.0007
(3, 2)	−4.0666	−4.4254	−0.3588	0.0002
(4, 3)	−4.1788	−4.6651	−0.4863	0.0001
(5, 4)	−4.4816	−4.5206	−0.0390	0.0000
(6, 5)	−4.3750	−4.3993	−0.0242	0.0003
(1, 2)	−4.3558	−4.4554	−0.0997	0.0003
(2, 3)	−4.4151	−4.5674	−0.1523	0.0004
(3, 4)	−4.4388	−4.5727	−0.1339	0.0001
(4, 5)	−4.4506	−4.4477	0.0029	0.0029
(5, 6)	−4.3854	−4.4880	−0.1026	0.0001

Figure 6 shows the band structures of the novel SWNTs with the Fermi level (E_F) at 0 eV. From Fig. 6, we can see that, for novel SWNTs in the Brillouin zone, besides (0, 2) and (4, 5), the valence bands and the conduction bands intersect near E_F, thus showing metallic properties. Furthermore, because the (0, 2) and (4, 5) SWNTs have very small indirect and direct band gaps, respectively, at room temperature, the electron can easily gain more energy and jump to the conduction band; thus, these SWNTs can also be regarded as metallic in properties. The valence bands and conduction bands near E_F of SWNTs with the same chirality indices converge toward the E_F gradually as the diameter is increased.

To further investigate the electronic properties of the novel SWNTs, we calculate the DOS of the novel SWNTs when E_F is set to 0 eV. It can be seen from Figure 7 that within the diameter range of our study, except SWNTs (5, 6) and (6, 5), for small diameters such as (0, 2), (2, 1), and (1, 2), the main orbital electrons near E_F are s-orbital, which means that almost no p-orbital electrons are present in the energy band near E_F. However, for larger diameters, p-orbital electrons are major contributors near E_F, while the contribution of s-orbital electrons approaches zero. Only some peaks appear below −5 eV and above 5 eV. Thus, these results indicate that no s-orbital electrons are in the energy bands near E_F in large-diameter SWNTs.

The DOS is the refinement of the band structure. Moreover, Figure 7 shows that the DOS near the E_F is not zero, which is consistent with the results of band structure, and further demonstrates that the novel SWNTs are all metallic.

4 Summary

Inspired by the SWNTs obtained from double-layer graphene or double-layer BN nanosheets by electron-beam engineering and by the successful preparation of graphene-like nanoribbons embedded with periodic four- and eight-membered rings, we explore the stability and electronic properties of novel SWNTs embedded with periodic four- and eight-membered rings in order to provide a guide for experimental preparation. Similar to six-membered ring SWNTs, these novel SWNTs can be regarded as curls of graphene embedded with periodic four- and eight-membered rings along different chirality indices. Based on this perspective, we first study the five novel SWNTs with different chirality indices and tube diameters. Using hydrogen passivation, a stable configuration satisfying thermodynamic requirements without imaginary frequencies is obtained. Secondly, according to the periodicity of the tubular clusters, novel

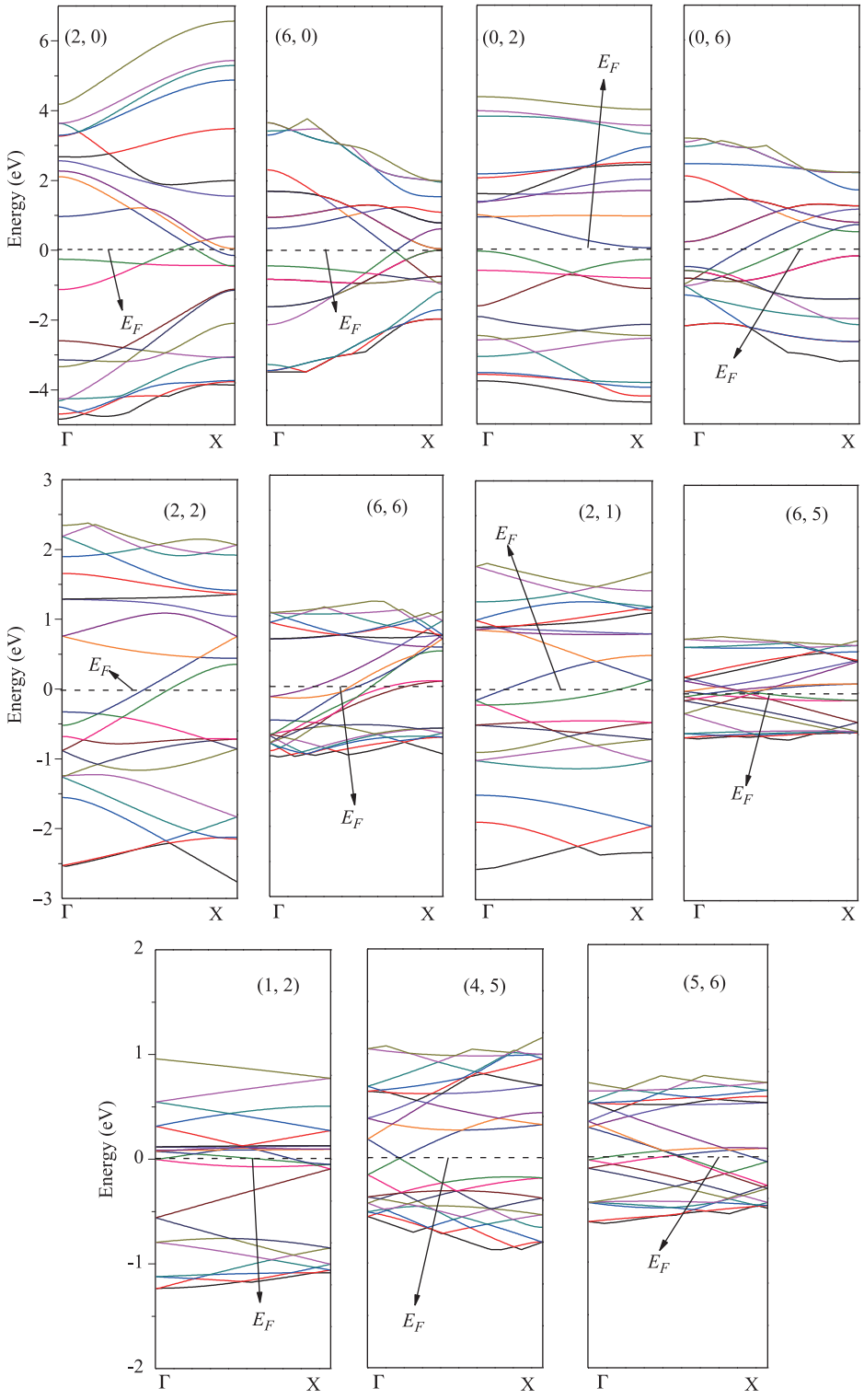

Fig. 6 The (2, 0), (6, 0), (0, 2), (0, 6), (2, 2), (6, 6), (2, 1), (6, 5), (1, 2), (4, 5), and (5, 6) band structures.

SWNTs are obtained by the PBC method with the smallest repeating units, which are intercepted from the corresponding tubular clusters. Research on the stability and electronic properties indicates that the stability of the novel SWNTs is unrelated to the chirality indices, but is related to the SWNT diameter. Larger diameters correspond to more stable novel SWNTs. We also find that the electronic properties of the novel SWNTs are

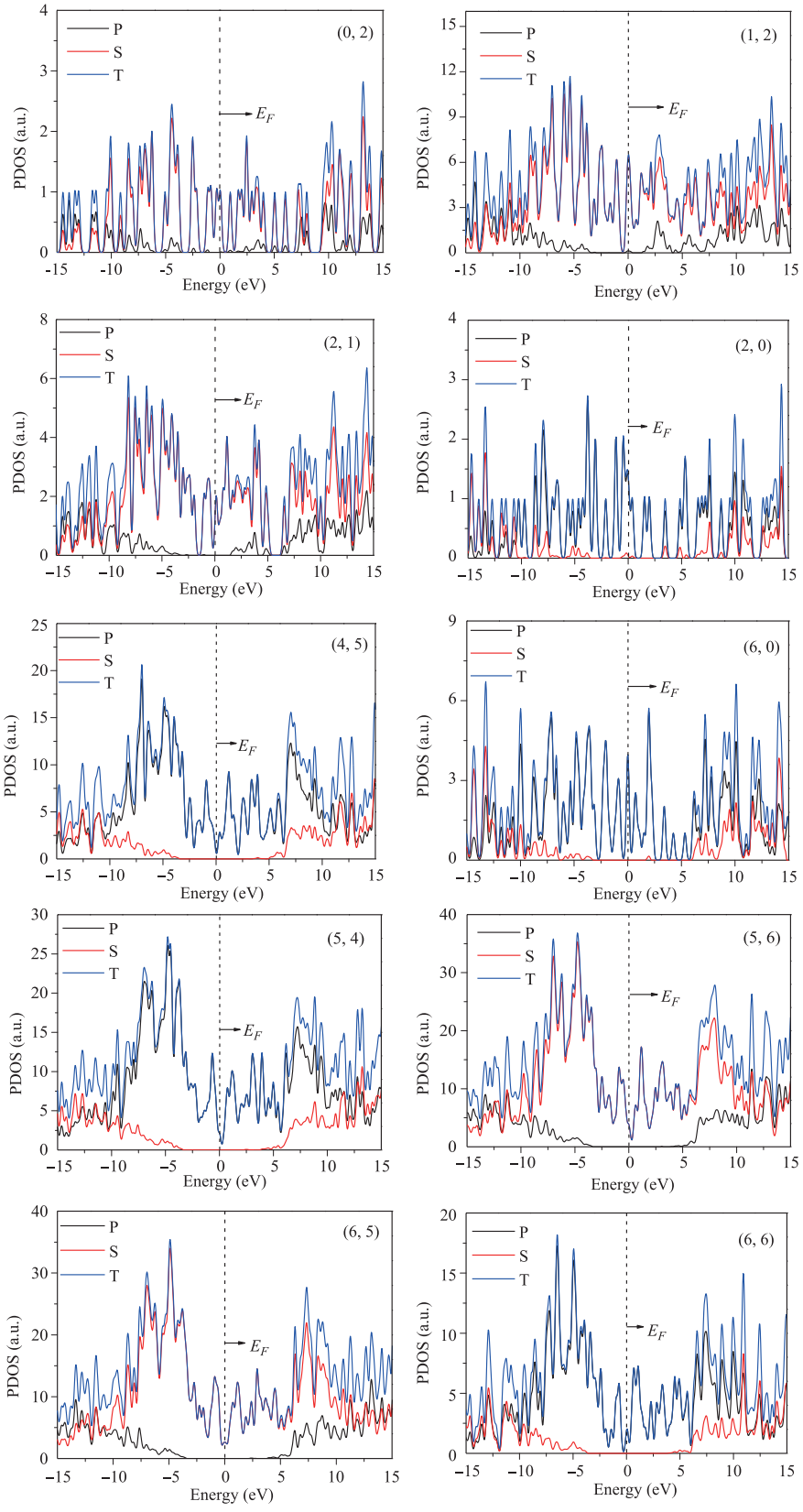

Fig. 7 The state density distribution of $(0,2)$, $(1,2)$, $(2,1)$, $(2,0)$, $(4,5)$, $(6,0)$, $(5,4)$, $(5,6)$, $(6,5)$, and $(6,6)$. Prepresents the p-orbital electron distribution, S represents the s-orbital electron distribution, Trepresents the total electron distribution, respectively.

independent of both the chirality indices and diameter; all the novel SWNTs show metallic properties. Our results provide a theoretical reference for the experimental preparation of SWNTs with single-type electronic properties. This would provide better selection for the research of quantum phenomena in quasi-one-dimensional solid-state model systems and promote the application of m-SWNTs.

Acknowledgements The authors acknowledge the financial support from the National Natural Science Foundation of China (Grant No. 11464044), the Foundation of Key Laboratory of Mineral Luminescent Material and Microstructure of Xinjiang (Project No. KWFG1701), and the "13th Five-Year" Plan for Key Discipline Physics Bidding Project, Xinjiang Normal University.

References

1. S. I. Yengejeh, S. A. Kazemi, and A. Öchsner, Advances in mechanical analysis of structurally and atomically modified carbon nanotubes and degenerated nanostructures: A review, *Compos. Part B Eng.* 86, 95 (2016)
2. Y. Cao, S. Cong, X. Cao, F. Wu, Q. Liu, M. R. Amer, and C. Zhou, Review of electronics based on single-walled carbon nanotubes, *Top. Curr. Chem.* 375(5), 75 (2017)
3. F. Yang, X. Wang, D. Zhang, J. Yang, D. Luo, Z. Xu, J. Wei, J. Q. Wang, Z. Xu, F. Peng, X. Li, R. Li, Y. Li, M. Li, X. Bai, F. Ding, and Y. Li, Chirality-specific growth of single-walled carbon nanotubes on solid alloy catalysts, *Nature* 510(7506), 522 (2014)
4. Y. Tang, J. Lu, D. Liu, X. Yan, C. Yao, and H. Zhu, Structural derivative and electronic property of armchair carbon nanotubes from carbon clusters, *Journal of Nanomaterials* 2017 (2017)
5. J. Liu, J. Lu, X. Lin, Y. Tang, Y. Liu, T. Wang, and H. Zhu, The electronic properties of chiral carbon nanotubes, *Comput. Mater. Sci.* 129, 290 (2017)
6. Y. N. Liu, J. Z. Lu, H. J. Zhu, Y. C. Tang, X. Lin, J. Liu, and T. Wang, Derivative and electronic properties of zigzag carbon nanotubes, *Acta Physica Sinica* 66(9), 093601 (2017)
7. S. Liu and X. Guo, Functional single-walled carbon nanotube-based molecular devices, *Acta Chimi. Sin.* 71(04), 478 (2013)
8. I. V. Zaporotskova, N. P. Boroznina, Y. N. Parkhomenko, and L. V. Kozhitov, Carbon nanotubes: Sensor properties, a review, *Modern Electronic Materials* 2(4), 95 (2016)
9. M. Sheikhpour, A. Golbabaie, and A. Kasaeian, Carbon nanotubes: A review of novel strategies for cancer diagnosis and treatment, *Mater. Sci. Eng. C* 76(November), 1289 (2017)
10. M. V. Chernysheva, E. A. Kiseleva, N. I. Verbitskii, A. A. Eliseev, A. V. Lukashin, Y. D. Tretyakov, S. V. Savilov, N. A. Kiselev, O. M. Zhigalina, A. S. Kumskov, A. V. Krestinin, and J. L. Hutchison, The electronic properties of SWNTs intercalated by electron acceptors, *Physica E* 40(7), 2283 (2008)
11. T. Tanaka, H. Jin, Y. Miyata, and H. Kataura, High-yield separation of metallic and semiconducting single-wall carbon nanotubes by agarose gel electrophoresis, *Appl. Phys. Express* 1(11), 1140011 (2008)
12. F. Zhang, P. X. Hou, C. Liu, B. W. Wang, H. Jiang, M. L. Chen, D. M. Sun, J. C. Li, H. T. Cong, E. I. Kauppinen, and H. M. Cheng, Growth of semiconducting single-wall carbon nanotubes with a narrow band-gap distribution, *Nat. Commun.* 7, 1 (2016)
13. I. Yahya, F. Bonaccorso, S. K. Clowes, A. C. Ferrari, and S. R. P. Silva, Temperature dependent separation of metallic and semiconducting carbon nanotubes using gel agarose chromatography, *Carbon* 93, 574 (2015)
14. H. Liu, Y. Feng, T. Tanaka, Y. Urabe, and H. Kataura, Diameter-selective metal/semiconductor separation of single-wall carbon nanotubes by agarose gel, *J. Phys. Chem. C* 114(20), 9270 (2010)
15. F. Yang, X. Wang, D. Zhang, K. Qi, J. Yang, Z. Xu, M. Li, X. Zhao, X. Bai, and Y. Li, Growing zigzag $(16, 0)$ carbon nanotubes with structure-defined catalysts, *J. Am. Chem. Soc.* 137(27), 8688 (2015)
16. F. Yang, X. Wang, M. Li, X. Liu, X. Zhao, D. Zhang, Y. Zhang, J. Yang, and Y. Li, Templated synthesis of single-walled carbon nanotubes with specific structure, *Acc. Chem. Res.* 49(4), 606 (2016)
17. H. Terrones, M. Terrones, E. Hernández, N. Grobert, J. C. Charlier, and P. M. Ajayan, New metallic allotropes of planar and tubular carbon, *Phys. Rev. Lett.* 84(8), 1716 (2000)
18. L. P. Biró, G. I. Márk, Z. E. Horváth, K. Kertész, J. Gyulai, J. B. Nagy, and P. Lambin, Carbon nanoarchitectures containing non-hexagonal rings: "necklaces of pearls, *Carbon* 42(12–13), 2561 (2004)
19. S. Zhang, J. Zhou, Q. Wang, X. Chen, Y. Kawazoe, and P. Jena, Penta-graphene: A new carbon allotrope, *Proc. Natl. Acad. Sci. USA* 112(8), 2372 (2015)
20. C. Liu and H. M. Cheng, Controlled growth of semiconducting and metallic single-wall carbon nanotubes, *J. Am. Chem. Soc.* 138(21), 6690 (2016)
21. G. Algara-Siller, A. Santana, R. Onions, M. Suyetin, J. Biskupek, E. Bichoutskaia, and U. Kaiser, Electron-beam engineering of single-walled carbon nanotubes from bilayer graphene, *Carbon* 65, 80 (2013)
22. T. Xu, Y. Zhou, X. Tan, K. Yin, L. He, F. Banhart, and L. Sun, Creating the smallest BN nanotube from bilayer H-BN, *Adv. Funct. Mater.* 27(19), 1603897 (2017)
23. M. Liu, M. Liu, L. She, Z. Zha, J. Pan, S. Li, T. Li, Y. He, Z. Cai, J. Wang, Y. Zheng, X. Qiu, and D. Zhong, Graphene-like nanoribbons periodically embedded with four- and eight-membered rings, *Nat. Commun.* 8, 1 (2017)

24. Y. L. Wang, K. H. Su, and J. P. Zhang, Studying of B, N, S, Si and P Doped (5, 5) carbon nanotubes by the density functional theory, *Adv. Mat. Res.* 463–464, 1488 (2012)
25. C. Garau, A. Frontera, D. Quiñonero, A. Costa, P. Ballester, and P. M. Deyà, Structural and energetic features of single-walled carbon nanotube junctions: A theoretical *ab initio* study, *Chem. Phys.* 303(3), 265 (2004)
26. J. Bai, X. C. Zeng, H. Tanaka, and J. Y. Zeng, Metallic single-walled silicon nanotubes, *Proc. Natl. Acad. Sci. USA* 101(9), 2664 (2004)
27. L. Guo, X. Zheng, C. Liu, W. Zhou, and Z. Zeng, An *ab initio* study of cluster-assembled hydrogenated silicon nanotubes, *Comput. Theor. Chem.* 982, 17 (2012)
28. M. S. Alam, F. Muttaqien, A. Setiadi, and M. Saito, First-principles calculations of hydrogen monomers and dimers adsorbed in graphene and carbon nanotubes, *J. Phys. Soc. Jpn.* 82(4), 1 (2013)
29. L. Qi, J. Y. Huang, J. Feng, and J. Li, In situ observations of the nucleation and growth of atomically sharp graphene bilayer edges, *Carbon* 48(8), 2354 (2010)
30. J. Y. Huang, F. Ding, B. I. Yakobson, P. Lu, L. Qi, and J. Li, In situ observation of graphene sublimation and multi-layer edge reconstructions, *Proc. Natl. Acad. Sci. USA* 106(25), 10103 (2009)
31. D. W. Boukhvalov and M. I. Katsnelson, Chemical functionalization of graphene, *J. Phys.: Condens. Matter* 21(34), 344205 (2009)
32. A. R. Botello- Méndez, E. Cruz-Silva, F. López-Urías, B. G. Sumpter, V. Meunier, M. Terrones, and H. Terrones, Spin polarized conductance in hybrid graphene nanoribbons using 5–7 defects, *ACS Nano* 3(11), 3606 (2009)
33. Q. Q. Dai, Y. F. Zhu, and Q. Jiang, Electronic and magnetic engineering in zigzag graphene nanoribbons having a topological line defect at different positions with or without strain, *J. Phys. Chem. C* 117(9), 4791 (2013)
34. X. Peng and R. Ahuja, Symmetry breaking induced bandgap in epitaxial graphene layers on SiC, *Nano Lett.* 8(12), 4464 (2008)
35. S. Reich, L. Li, and J. Robertson, Structure and formation energy of carbon nanotube caps, *Phys. Rev. B* 72(16), 1654231 (2005)
36. S. Singh and A. H. Romero, Giant tunable rashba spin splitting in a two-dimensional BiSb monolayer and in BiSb/AlN heterostructures, *Phys. Rev. B* 95(16), 165444 (2017)